A Study of the Effect of Homogenisation Conditions on Recrystallisation in the Al-Mg-Mn Alloy AA5454

M. Osman[1], O. Engler[2], K. Karhausen[2], L. Löchte[2] and A.J. McLaren[1*]

[1] Department of Mechanical Engineering, University of Strathclyde, 75 Montrose Street, Glasgow, G1 1XJ, Scotland, UK

[2] Hydro Aluminium Deutschland GmbH, R & D Centre Bonn, P.O. Box 2468, D–53014 Bonn, Germany

Keywords: AA5454, homogenisation, recrystallisation, precipitate distribution.

Abstract.

The purpose of the present work is to understand the microstructure development and, particularly, to control the progress of recrystallisation in hot strip in the Al-Mg-Mn alloy AA 5454, which is typically used for the manufacture of structural automotive components. The chemical composition, together with the thermomechanical processing history of this material have a strong influence on the microstructure of the product and the ensuing properties as it is supplied to the customer. Electrical conductivity measurements, thermal analysis and electron microscopy have been carried out in order to characterise the evolution of precipitation state at various stages in the processing route. The conditions of the homogenisation heat treatment have been varied, and the effect on subsequent recrystallisation after hot rolling has been evaluated in both the as-cast and rough-rolled condition by optical microscopy techniques. Results indicate that the conditions of homogenisation heat treatment and roughing rolling are critical for the generation of a suitable recrystallised microstructure in AA 5454 hot strip. A new two-stage homogenisation practice has been developed to expedite post-rolling recrystallisation in this alloy.

* corresponding author
phone +44 141 548 3104, Fax: +44 141 552 5105, E-mail: Andrew.McLaren@strath.ac.uk

1. Introduction

The material studied in this work is the Al-Mn-Mg alloy AA5454 which is typically used for the manufacture of structural automotive components.[1,2] For many structural applications, the material is supplied to the automotive manufacturer in the form of hot rolled coil, in a thickness range of 3 to 10 mm. The process route for the alloy involves DC (direct chill) casting, followed by homogenisation heat treatment. The alloy is then reverse hot rolled in the temperature range around 500°C from an initial thickness of 600mm to approximately 30mm. The resulting rough-rolled transfer slab is further reduced in three or four tandem passes to final thickness. The hot band is coiled and allowed to cool down within 24 to 48h to ambient temperature. During this time at elevated temperature the coiled hot strip may recrystallise, which is commonly referred to as "self annealing". Thus, for a given composition, the thermomechanical processing history of the alloy controls the microstructure and the resulting properties of the product as it is supplied to the customer.

Most automotive structural applications require materials with good formability. However, under certain processing conditions, significant portions of the material are observed to consist of grains highly elongated in the direction of rolling, mixed with small equiaxed grains. This partially recrystallised structure is considered to be undesirable due to its adverse effects on ductility and formability. The purpose of the present work is to understand the underlying mechanisms that control the microstructure of the alloy, by characterisation of the evolution of precipitate species and their effect on static recrystallisation. The effect of segregations of recrystallisation-inhibiting elements is assessed. Furthermore, the impact of the preheating treatment on the particle state of the as-cast ingot is analysed. It is known that a suitable homogenisation cycle may strongly improve the down stream recrystallisation.[3-6] A modified homogenisation practice is proposed which results in a particle state that facilitates recrystallisation during self-annealing of the coiled hot strip.

2. Experimental Procedure

The material used in the present study is the Al-Mg-Mn alloy AA 5454 with an average chemical composition as shown in Table 1. The AA standard chemical composition of this alloy is given in the same table for comparison. The material has been examined in two conditions. As-cast material was obtained in the form of 15mm thick slices cut across the original DC cast ingot. Transfer slab material was obtained after the reversible rough rolling

passes. The rough-rolled material was supplied in the form of 1300mm wide and 28mm thick plate.

Because of the chemical heterogeneity that was expected to result from the solidification process, the spatial distribution of some of the elements (Mg, Mn, Fe, Si and Cr) was also examined through the rough-rolled plate thickness by means of optical emission spectrometry, OES. A relatively large spot diameter of 30mm was used so as to average and minimise the measurement errors.

The importance of the conditions of pre-rolling homogenisation heat treatment was examined with emphasis on the rate of subsequent static recrystallisation. Rolling slabs 120mm in length and 50mm in width were cut from along the rolling direction from the supplied rough-rolled transfer slab. Various pre-heating treatments were applied prior to hot rolling so as to study the impact of the homogenisation practice on particle state as well as elements in solid solution. Besides analysis of the standard isothermal one-stage pre-heating, a new two-stage homogenisation practice was developed that facilitates recrystallisation of the hot rolled material.

The rolling trials were carried out on a small-scale laboratory mill, with roll diameter 135mm. In a first set of rolling trials, the impact of pre-heating cycle on the subsequent recrystallisation behaviour was investigated. The temperature during heat treatment and rolling was monitored by a K-type thermocouple, which was inserted to the geometric centre of the rolling slab, its output being recorded by a PC-based data acquisition system. In this set of experiments, the samples were homogenised for different times (6 to 18 hours) at different temperatures (540 to 585°C), and then cooled down to a rolling temperature of 400°C or 486°C. Finally, the material was rolled in one pass of 36 or 50% thickness reduction (corresponding to an equivalent strain of ε=0.52 or 0.8), followed by water quenching. The strain rate varied from 2.5 to 6.8 s^{-1}.

After determining the optimum pre-annealing conditions, samples of both as-cast and rough-rolled material were subjected to a more complex three pass hot rolling schedule with a total strain of 1.36 so as to mimic the three final passes of industrial tandem rolling. Because of the limitations of the laboratory mill with regard to temperature control and the strain rates achievable, the industrial processing schedules could not be reproduced precisely in the

laboratory. Therefore, the microstructure evolution during the commercial three-stand tandem rolling practice was simulated by choosing values of temperature, T_D and strain rate, $\dot{\varepsilon}$ which gave the same mean value of the Zener-Hollomon parameter as that expected during the industrial rolling. The Zener-Hollomon parameter, Z, is essentially a temperature compensated strain rate, and is given by:

$$Z = \dot{\varepsilon} \exp\left(\frac{Q}{RT_D}\right) \quad (1)$$

Where R is the Gas Constant ($8.31 Jmol^{-1}K^{-1}$), and Q: is an apparent activation energy which was chosen as $156 kJmol^{-1}$.

Since the temperature of the rolled slab changes during the rolling process, the Sheffield Leicester Integrated Model for Microstructural Evolution in Rolling (*SLIMMER)* finite difference software,[7] was used to simulate the slab temperature profiles through the three rolling passes and determine the entry temperature of the first pass to give the same mean Z value as in industrial tandem rolling. The small size of the rolled slabs and consequently the higher chilling effect of the lower temperature laboratory rolls compensate for the effect of performing the rolling with a lower strain rate of about $5\ s^{-1}$.

After rolling, the slabs were immediately quenched to room temperature in a water bath. Sections cut from the central portion of the rolled slabs were annealed at 325 or 345°C for various times, t, and subsequently examined to evaluate the progress of static recrystallisation. The recrystallised volume fraction $X(t)$ was measured by standard optical microscopy methods. Differential thermal analysis (DTA), differential scanning calorimetry (DSC), and transmission electron microscopy (TEM) were conducted to evaluate the processes of precipitation and dissolution of second-phase during heat treatment under different conditions. Measurements of electrical conductivity / resistivity were carried out in liquid helium at 4.2 K by means of the four-point method, utilising measurements of potential drop across the sample.

3. Experimental Results

3.1. Microchemistry

As already described in the introduction, the alloy under investigation has a relatively high content of alloying elements. Segregation of these elements would strongly affect the

recrystallisation behaviour in different locations throughout the rolled sheet. Therefore, the spatial distribution of the elements Mg, Mn, Fe, Si and Cr was measured by OES. The expected symmetry about the plate principal axes reduces the number of the measurement points by a factor of four since one-quarter of the plate cross section only is analysed. Fig. 1a. shows the region of the slab analysed, relative to the cross section. A grid of 4 points along the Y axis and 6 positions along the X axis was designed to cover the scanned area. Table 2 lists the extreme values of the alloy composition obtained, which are compared to the mean composition given in Table 1. Compared to the as-cast ingot the segregation profiles appeared to be largely unchanged.

Fig. 1b and 1c show the distribution contours of the elements Mg and Cr, respectively. Mn is distributed fairly uniformly with only minor variation in different regions of the plate, whereas most species, most notably Mg, are segregated towards the outer regions of the plate (Fig. 1b). In contrast, Cr is found preferably in the core of the plate/ingot, (Fig. 1c). Thus, combining the effects of the recrystallisation-inhibiting species Mn and Cr with that of the recrystallisation-promoting Mg, it would appear that recrystallisation in the centre layers should be delayed as compared with the outer regions.

3.2. Thermal analysis

Differential scanning calorimetry (DSC) was employed to study the critical temperatures corresponding to the different precipitation / dissolution reactions and to determine the solidus temperature of the alloy. A sample was taken from the outer parts of the as-cast ingot with maximum Mg content (see Fig. 1b). The sample was heated with a heating rate of 50°Cmin^{-1} up to 750°C; the results are plotted as a function of temperature in Fig. 2a. Both the DSC curve (full line) and its time derivative, *d*DSC/*dt* (dashed line), are shown. These results suggest that during heatment in the entire temperature range from 250°C to 570°C precipitation reactions take place, with three distinct exothermic peaks at 290°C, 450°C and 550°C. Between 581°C and 660°C a strong endothermic reaction is observed, which is attributed to sample melting. Thus, the solidus temperature of the present alloy is approximately 581°C. After a homogenisation anneal, the DSC curves remained largely unaffected, yet the solidus temperature is raised slightly to 583°C.

The precipitation / dissolution behaviour of the rough-rolled material was examined by means of differential thermal analysis (DTA). Samples from positions corresponding to the extremes

of the inhomogeneous composition (i.e. maximum and minimum contents of Fe, Mg and Si) were analysed and their behaviour is shown in Fig. 2b. The samples were heated up to 700°C with a heating rate of 10°Cmin^{-1} and held at this temperature for 1 hour before cooling with the same rate. For better scale presentation, results are shown up to 600°C only. During heating, both samples show endothermic reactions over a wide range of temperatures with a single peak at 556°C (position A). The peak intensity changes with composition in that a stronger peak is observed as the solute concentration increases. Note that the DTA curves of the rough-rolled samples show a different behaviour from than observed in the DSC analysis of the as-cast material, where below the solidus temperature exothermic reactions, i.e. *formation* of particles, were observed. This difference may be attributed to the fact that the rough-rolled material had undergone a homogenisation treatment already. The precipitates that had formed during the previous pre-heating cycle re-dissolve at sufficiently high temperatures. Thus, the DTA measurements provide useful information on the temperature regime required to dissolve particles.

During cooling, an exothermic reaction corresponding to the re-precipitation of the second phases in a narrow temperature range is observed (position B). Interestingly, the peak temperature is slightly *higher* than that reported for dissolution, while because of nucleation restrictions re-precipitation of the dissolved phases is generally expected to take place at a *lower* temperature. This discrepancy can presumably be explained by the much higher cooling rate applied during DTA than that prevailing in a large DC cast ingot. Several authors, [8-10] reported the formation of different phases as the cooling rate changes. They reported a cooling rate of <1°Cs^{-1} for the formation of Al_3(Mn,Fe), 1-10°Cs^{-1} for the Al_6(Mn,Fe) and 8-10°Cs^{-1} for the α phases $Al_{12}(Mn,Fe)_3Si$ and $Al_{15}(Mn,Fe)_3Si_2$.

Exceeding the solidus temperature during the homogenisation cycle causes a partial melting of the material. After re-solidification this may lead to the formation of eutectic phases on the grain boundaries. An example of this behaviour in a slab homogenised at 600°C is shown in Fig. 3a. During subsequent rolling, these brittle phases may initiate crack formation within the plate (Fig. 3b). Furthermore, homogenisation temperatures in excess of 590°C gave rise to massive grain growth.[11]

3.3. Electrical conductivity

Detailed measurements of the electrical conductivity were carried out to evaluate the impact of the homogenisation temperature, soaking time and the subsequent cooling rate on the precipitation/dissolution of the secondary phases during the pre-heating cycle. Small specimens taken from the outer regions of the as-cast ingot were homogenised for 16 hours at temperatures of 480, 500, 520, 540, 560 and 575°C, after which they were water quenched (isothermal single-stage treatment). Fig. 4 shows the measured values of electrical conductivity, plotted against soaking temperature (open circles). A few specimens were subjected to either a shortened or prolonged annealing cycle, the corresponding conductivity data are plotted with symbols + and x, respectively. For comparison, the conductivity of a non-annealed as-cast sample was determined as well. The as-cast structure revealed a very low conductivity of 23.8 MS/m (= 23.8 m/Ωmm^2), which implies that a large amount of alloying elements is in supersaturated solid solution.

The conductivity data of Fig. 4 are to be compared with the expected equilibrium value as a function of soaking temperature. As described in detail by Altenpohl,[12] the equilibrium conductivity $\sigma(T)$ can be derived from the relationship between electrical conductivity and the solid solution content in equilibrium. For dilute alloys, the changes in electrical resistivity, ρ, scale linearly with the contents of alloy elements in solid solution, c_i (in wt%):

$$\sigma(T) = \frac{1}{\rho_{Al} + 0.0055 \cdot c_{Mg} + 0.0383 \cdot c_{Mn} + 0.032 \cdot c_{Fe} + 0.0065 \cdot c_{Si} + 0.042 \cdot c_{Cr}} \quad [\text{MS/m}] \quad (2)$$

The specific resistivity of aluminium, ρ_{Al}, was fitted such that the resulting curve matches the highest data points in Fig. 4. The resulting value, $\rho_{Al} = 20$ Ωcm, corresponds roughly to the resistivity of 6N aluminium at 4.2K, while minor deviations can be ascribed to the additional alloying elements (in particular, Cu) and impurities. As a lower bound solution, the nominal alloy composition from Table 1 was introduced in Eq. (2), yielding an electrical conductivity of σ_{ss}=15.2 MS/m. This number represents the minimum conductivity obtained if *all* alloying elements were retained in solid solution.

For the calculation of the equilibrium solute levels c_i of the various species as a function of temperature the *CALPHAD* approach (*CAL*culation of *PH*ase *D*iagrams,[13,14]) has been used

together with the commercial software package *FactSage*^{TM}.[15] For aluminium alloys many of the required data have been determined in the framework of the EU funded programme COST 507 and published in a thermodynamic database.[16] In the present study an extended data base was used, including more alloying elements, with special focus on the aluminium-rich corner.[17]

In general, an increase in the quantity of solutes in the matrix causes a decrease in electrical conductivity, σ.[12] This is shown by the steady reduction in measured conductivity as homogenisation temperature is increased (Fig. 4). However, it is noted that for the chosen annealing time of 16 h, the measured conductivity approaches the equilibrium value only after homogenisation at temperatures in excess of 560°C, whereas the samples annealed at temperatures below 550°C are still away from the equilibrium curve $\sigma(T)$.

To study the effect of changing the soaking time, specimens were homogenised for 7 h at 540°C and for 80 h at 520°C, respectively. The measured conductivity of the specimen homogenised for shorter times at 540°C was only slightly lower than that of the sample homogenised for 16 h at the same temperature. From the opposite point of view, this implies that extending the soaking period from 7 to 16 h has a relatively small effect on changing the precipitation / dissolution state.

In contrast, homogenisation for longer periods (80 h) increased the measured conductivity remarkably; actually, values close to the equilibrium conductivity were obtained. Thus, the – on first sight rather unsystematic – results of the isochronal annealings can be attributed to a combination of thermodynamics and kinetics of the solution / precipitation reactions. The rise in conductivity with time suggests a precipitation of the supersaturated solutes from the matrix rather than dissolving the pre-existing phases. This depletion of the matrix may take place either by growth of pre-existing particles or by precipitation of new phases. TEM investigations revealed that homogenisation at temperatures less than 540°C causes both additional formation of new fine precipitates and growth of the existing ones. In order to illustrate this point, Fig. 5a shows a TEM micrograph of the as-cast microstructure clear of the large constituent particles. The micrograph comprises one rhomboidal particle of about 0.5μm together with a number of rather inhomogeneously distributed small particles of 20-50 nm size. Fig. 5b shows the precipitation substructure after soaking for 6h at 540°C and

^{TM} *FactSage* is a trademark of GTT-Technologies GmbH, D-52134 Herzogenrath, Germany

subsequent water quenching. Compared to the as-cast state, the fraction of secondary particles as well as their average size increased significantly. Thus, during the "homogenisation" cycle massive precipitation takes place, and the resulting particle state is key to controlling the subsequent recrystallisation behaviour.

Extended soaking time had only limited influence on this precipitate distribution, but encourages additional grain boundary precipitation. The ensuing precipitation state would not facilitate recrystallisation, while the grain boundary precipitates would even decrease ductility. For this reason, it is preferable to carry out homogenisation for short times to avoid deleterious grain boundary precipitation, but adjust the precipitate distribution by other means, *viz*., by changes in the temperature cycle, in order to expedite microstructure development during self annealing.

In preparation for hot rolling, the homogenised ingots typically cool down considerably before rolling commences. To examine the impact of this cooling period on the state of precipitation / supersaturation, a specimen was homogenised for 6 h at 570°C and then furnace cooled within 2 h to a sub-homogenisation temperature of 480°C (two-stage treatment). Then, the sample was held for 3 h at this temperature and subsequently water quenched. This furnace cooled specimen (labelled A) showed a notably higher conductivity compared with the water quenched one (filled symbols in Fig. 4). Thus, cooling the homogenised material slowly was found to affect the precipitation state but, because of the shorter soaking time, the depletion of the solutes is expected to take place through growth of the pre-existing precipitates rather than the grain boundary precipitation. Another specimen (B) was subjected to the same heat treatment but cooled to a lower sub-homogenisation temperature of 450°C. In this specimen, the conductivity increased further.

3.4. Hot rolling experiments

As described in the experimental section, in a first set of rolling trials, the impact of homogenisation conditions on the subsequent recrystallisation behaviour was examined. Rolling slabs 50 mm wide and 120 mm long were cut along the rolling direction from the rough-rolled transfer slab. The slabs were homogenised for different times t_{hom} at different temperatures T_{hom}, and then cooled to the rolling temperature T_{roll}. Then the material was rolled in one pass of strain ε with strain rate $\dot{\varepsilon}$, followed by water quenching. The test matrix of hot rolling experiments is given in Table 3.

In order to examine the recrystallisation kinetics, the hot rolled samples were annealed for various times t in a salt bath at either 325°C or 345°C, and the recrystallised volume fraction $X(t)$ was assessed by standard light optical methods. The annealing times that are necessary to achieve 50% recrystallisation, labelled as $\tau_{50\%}$, are included in Table 3. Note that all kinetics data described in this section were obtained from the one-quarter position through the thickness of the hot rolled specimens. In the centre layer, recrystallisation advanced much slower, by contrast. This is presumably caused by the inhomogeneous distribution of strain and temperature during hot rolling through the thickness of the slab. Furthermore, the recrystallisation in the sheet centre may also be retarded by the macro-segregation of the recrystallisation-inhibiting species Cr towards the centre; while recrystallisation-promoting Mg is preferably found in the outer layers (see Fig. 1). Nonetheless, the relative changes of recrystallisation kinetics discussed hereafter are valid for the centre position as well, yet shifted to a longer time scale.

As an example of the resulting recrystallisation kinetics, Fig. 6 shows the development of the recrystallised fraction $X(t)$ as a function of time t for samples A1 and A2, where homogenisation cycle and annealing temperature have been varied. As expected, the higher annealing temperature led to faster recrystallisation (open symbols / dotted lines). However, the homogenisation practice, most notably, the rate of cooling from homogenisation temperature to rolling temperature, likewise had a strong impact on the progress of recrystallisation. Figure 7 shows a schematic representation of the tree cooling practices used in the current work. Here, "w.q" indicates specimens water quenched from the homogenisation temperature to room temperature, followed by subsequent reheating to the rolling temperature. The designations "f.c." and "a.c." indicate furnace and air cooling respectively from the homogenisation temperature directly to the rolling temperature. The specimens that were water-quenched and re-heated to rolling temperature (w.q.) revealed much slower recrystallisation kinetics than the samples that were slowly cooled in a furnace (f.c.) down to the rolling temperature. Air cooling (a.c.) of small, lab-sized specimens proceeds fairly rapidly (which is not true for large industrial ingots). Accordingly, air cooling gave rise to recrystallisation kinetics close to that of the water quenched samples.

Besides annealing temperature and cooling rate, the parameters of the pre-annealing cycle, *viz*., homogenisation time t_{hom} and temperature T_{hom}, appeared to affect the recrystallisation

kinetics strongly. In general, prolonged homogenisation time and, most notably, increased homogenisation temperature accelerated the progress of recrystallisation (samples A3-A8 in Table 3). These effects are summarised in Fig. 8, where the time for 50% recrystallisation, $\tau_{50\%}$, is plotted *vs*. the homogenisation temperature for two different homogenisation times and annealing temperatures.

With regard to the rolling parameters, increasing strain, ε, and strain rate, $\dot{\varepsilon}$, both accelerated recrystallisation considerably, with the latter being particularly pronounced in specimens at lower strains (samples A4 and A9-A11 in Table 3).

3.5. Simulation of the three tandem passes with an optimised homogenisation cycle

The aim of the present study is to facilitate recrystallisation during self-annealing of the coiled hot strip. With this in mind, the hot rolling experiments described in the previous section can be summarised as follows. Evidently, high strains and high strain rates both favour subsequent recrystallisation, yet there are obviously limitations as to the extent to which this can be utilised in industrial practice. Therefore, the pre-heating cycle has greatest potential to control and improve the progress of recrystallisation. Here, it appears that two points are of importance: (i) the homogenisation temperature should be high, preferably above 560°C (yet still below the alloy's solidus temperature of ~580°C); (ii) in preparation for hot rolling, the material should be cooled slowly (furnace cooling) to the rolling temperature ranging from 400 to 500°C.

Based on the hot rolling experiments and supported by thermal analysis plus electrical conductivity measurements, a novel two-stage homogenisation practice was developed and compared with a conventional one-stage treatments represented in Fig. 7. These experiments were performed with both as-cast and rough-rolled material. It must be emphasised that both routes have their drawbacks in simulating the industrial rolling practice: with as-cast material the total rolling deformation is much lower than that applied in reality, while starting with rough-rolled samples implies that the material has already been subjected to the industrial pre-heating prior to rough-rolling, which will affect the particle state introduced through the additional lab homogenisation treatment.

The new homogenisation cycle was comprised of soaking for 6h at 560°C, furnace cooling to a temperature of 400°C and holding for about one hour before hot rolling (sample B1 in Table

3). This temperature cycle was chosen in order to dissolve as much as possible of the fine intermetallic particles during the first stage and to accelerate coarse precipitation away from the grain boundaries during the second. For comparison, another sample was homogenisation annealed for 6h at 540°C, followed by (fairly rapid) air cooling to a rolling temperature of 486°C (single-stage homogenisation; sample B2).

Fig. 9 compares the observed distribution of second-phase particles in two differently homogenised samples taken from the rough-rolled slab. The material homogenised at 540°C according to the single-stage cycle shows a rather uniform distribution of particles with sizes of about 0.1 μm (Fig. 9a), which are most likely to adversely affect recrystallisation after subsequent hot rolling. The two-stage homogenisation practice evidently increased the size of the particles, as well as their mean separation (Fig. 9b). This should reduce their ability to pin grain boundaries during post-rolling heat treatment and, hence, enhance the kinetics of recrystallisation.

The impact of the optimised homogenisation treatment on the resulting microstructure and degree of recrystallisation has been assessed after the experimental simulation of the industrial three-stand tandem mill for both the as rough rolled and as cast condition. As outlined in the experimental section, specimens with the two different homogenisation treatments were rolled for three passes with a total strain of 1.36 at a strain rate of $5s^{-1}$ so as to mimic the three passes of tandem rolling. Finally, the samples were recrystallisation annealed.

Fig. 10a. shows the microstructure of a sample of rough rolled material which had experienced the single-stage homogenisation for 6 h at 540°C, followed by simulated tandem rolling and recrystallisation anneal. The microstructure consists of recrystallised grains aligned in bands, separated by unrecrystallised grains that are highly elongated parallel to the rolling direction. The recrystallised grains are not equiaxed. They appear to nucleate in the vicinity of coarse particles that stimulate their nucleation. Fig. 10b. shows the microstructure of a sample of as cast material, homogenised, rolled and annealed under identical conditions to that of the rough rolled slab represented in fig. 10a. The microstructure heterogeneity was found to be more severe in the slab originally in the as-cast condition, where the coarse primary precipitates are less uniformly distributed.

Fig. 11 shows a TEM micrograph taken at the centre of the same sample as that shown in fig. 10. The micrograph shows small second-phase precipitates, with diameter less than 0.1μm and aspect ratio of 2, which appear to pin subgrain boundaries within the unrecrystallised grains. As a result, the formation of recrystallisation nuclei is likely to be retarded in these regions.

Fig. 12 shows the microstructure of the as rough rolled slab which has been homogenised according to the new two-stage process. In this case, despite the lower annealing temperature and shorter annealing time, the material is fully recrystallised with a uniform equiaxed grain size. This indicates that the two-stage homogenisation treatment gives greatly enhanced control over the microstructure of the alloy.

4. Discussion

Most automotive applications of AA 5454 hot band consist of rather complex structures, the production of which requires quite large plastic strains. This evidently requires a high ductility and good formability, which means that proper control of the microstructure of the material is key to achieving the required product properties. Thus, the thermomechanical processing history of the alloy must be controlled such that the hot band is delivered to the customer in a fine-grained soft state, which implies that the material preferably recrystallises upon cooling of the coiled hot band, that is, during "self-annealing". As an alternative to self annealing, a separate furnace annealing stage can be used after rolling. This is likely to achieve good results but introduces a significant extra cost to the material production process.

The hot rolling trials performed in the course of the present study have substantiated that high strains and high strain rates both favour subsequent recrystallisation (Table 3). As a matter of fact, this has been utilised in industrial practice, yet there are obvious practical limitations as to the extent to which this can be used to improve recrystallisation. The focus of this work has therefore been on the pre-heating cycle which has the highest capability of controlling and improving the progress of recrystallisation during self-annealing.

The recrystallisation of Al alloys is largely controlled by the precipitation state of the material. It is well established that coarse, micron-sized particles may promote recrystallisation through particle stimulated nucleation (PSN).[18] Small sub-micron particles

retard the material's softening, however, since they interact with dislocations and/or sub-boundaries during recovery and with the moving grain boundary during recrystallisation (e.g. Fig. 11).[19-22] Accordingly, it appears that both the primary constituents and fine secondary precipitates will have a strong influence on the development of microstructure during processing of this alloy. However, dissolved elements may likewise affect recrystallisation kinetics by reducing grain boundary mobility through the mechanism of solute drag.[23,24]

During the industrial processing of Al alloys the precipitation state is largely governed by the cooling of the as-cast slab and the subsequent homogenisation cycle. In preparation for the hot rolling, the DC cast ingots often receive a simple pre-heating to the subsequent rolling temperature of 450-500°C, which is generally too low for significant precipitation / dissolution reactions to take place. Alternatively, the ingots are heated to a higher temperature between 500°C and 600°C, in a cycle which may last up to 48 h. During this homogenisation cycle short-range intercellular segregation (coring) is reduced, large, irregularly shaped constituents are spheroidised and soluble phases in the material are dissolved. Then, the ingots are allowed to cool down to a rolling temperature in the range 400 to 500°C before hot rolling commences. The hot rolling experiments summarised in Table 3 indeed reveal a pronounced impact of the pre-heating parameters on the progress of recrystallisation; here, presented in terms of the time $\tau_{50\%}$ necessary to achieve 50% recrystallisation.

Because of the massive application of chilling water the DC cast slabs cool down rapidly .[25,26] Even in the core of a 600 mm thick slab the cooling rates exceed $1°Cs^{-1}$, and in the outer parts they may reach as much as $10°Cs^{-1}$. This implies that the temperature range of 450-600°C being most important for precipitation reactions is passed within fractions of a minute to a maximum of a few minutes, which is much too short for equilibrium-precipitation reactions to be achieved. In the present study this fact is substantiated by measurements of the electrical conductivity, σ (Fig. 4). The as-cast material revealed a rather low conductivity of 23.8 MS/m, and all pre-heating cycles examined raised the conductivity to values ranging from 31 to 39 MS/m. On the other hand, the conductivity of the as-cast slab is notably higher than the lower bound value derived under the assumption that *all* elements of the nominal alloy composition were retained in solid solution, σ_{SS} = 15.2 MS/m.

Transferred to the precipitation state these values indicate that the as-cast slab is in a supersaturated state with only incomplete precipitation well away from equilibrium, which

may be attributed to the slow diffusion of Mn dominating the homogenisation procedure.[3] Thus, during the "homogenisation" cycle massive precipitation may take place (e.g. Fig. 5). This observation is also in accord with the DSC measurements of the as-cast material (Fig. 2a), which showed several exothermic reactions in the temperature range from 250°C and 570°. In order to analyse the underlying precipitation reactions in more detail, thermodynamic calculations were performed with the program *FactSage* (see above). Fig. 13a shows the mass fraction x_i of the various equilibrium phases i as a function of temperature T for alloy AA 5454 in thermodynamic equilibrium. However, during heating of an as-cast ingot the starting point is a supersaturated non-equilibrium state. Following the method utilised by Scheil,[27] the resulting supersaturated particle state can be estimated through a solidification simulation where any diffusion in the solid state is frozen. The results, plotted in Fig. 13b, indicate that during solidification, only particles of the phase $Al_6(Mn,Fe)$ plus traces of $Al_3(Fe,Mn)$ form, while the precipitation of the α phases $Al_{12}(Mn,Fe)_3Si$ and $Al_{15}(Mn,Fe)_3Si_2$ is suppressed. Furthermore, it appears that at the solidus temperature of 581°C there is still some 10wt% of liquid phase left which, during rapid cooling to room temperature, will contribute to the supersaturation of the matrix. A combination of the particle state derived from Fig. 13b with the stability ranges of equilibrium phases in Fig. 13a permits indexing of the DSC peaks in Fig. 2a. Presumably, the peaks observed at 290°C, 450°C and 550°C can be ascribed to the precipitation of Mg_2Si, $Al_6(Mn,Fe)$ and α phases, respectively, while precipitation of the E-phase, $Al_{18}Cr_2Mg_3$, could not be discerned with DSC.

Zaidi and Sheppard,[3] have shown that an increase in homogenisation temperature decreased the recrystallisation temperature (i.e. temperature for 100% recrystallisation within a given time period; here, 1h) in AA 5252 and AA 5454. For the latter, they observed almost a step change in recrystallisation kinetics at about 550°C. This was attributed to dissolution of the Mg and Mn bearing phases in the as-cast slab. The electrical conductivity measurements of the present study confirm that at temperatures in excess of ~550°C the amount of solute alloying elements increased notably compared to lower soaking temperatures (Fig. 4). DTA analysis of the rough-rolled material validates maximum dissolution of phases at temperatures of about 550-560°C (Fig. 2b). Below 540°C these particles remain largely un-dissolved, in contrast. TEM investigations revealed additional precipitation of new fine phases plus growth of the existing ones, resulting in the rather uniform distribution of particles with sizes of less than 0.1μm shown in Fig. 5b. Also, soaking for longer times did not lead to dissolution of existing phases, but formation of deleterious grain boundary particles was observed.

In the case of a high temperature soaking practice, the material is usually allowed to cool down before hot rolling commences. The present hot rolling trials have shown that the rate of this cooling strongly influences the rate of the down stream recrystallisation. Engler *et al*.[6] have observed that, in AA 5083, varying the cooling rate from homogenisation temperature (500°C) changes the recrystallisation kinetics of cold rolled sheet by more than three orders of magnitude. Samples that cooled very slowly with a precipitation state close to equilibrium showed fastest recrystallisation, whereas increased cooling rates slowed down recrystallisation considerably. Measurement of the electrical conductivity during the progress of recrystallisation indicated that this delay was caused by the concurrent precipitation of supersaturated elements. Similar effects of solute elements on the progress of recrystallisation have been reported in other Mn containing alloys as well.[5, 22, 28]

Thus, with excessive cooling rates, like air cooling and, obviously, water quenching, alloying elements are retained in supersaturated solid solution, which then retard recrystallisation during self-annealing. However, with sufficiently low cooling rates, such as controlled furnace cooling, the solutes can precipitate. Because of the fairly high annealing temperatures – at least during the early stages of the cooling period – diffusion will be easy, leading to the formation of a rather coarse particle distribution that does not retard post-rolling recrystallisation to a great extent (e.g. Fig. 9b).

It must be emphasised here that the particle distribution shown in Fig. 9a and b may be somewhat misleading in that the rough-rolled material has previously seen another homogenisation cycle in the industrial plant (see above). In order to quantify the impact of this extra homogenisation plus the deformation during rough rolling, the evolution of the particle size distribution accompanying single and double-stage homogenisation for as-cast and rough-rolled specimens is compared in Fig. 14. Obviously, for the rough-rolled specimens there is a notable shift in the distribution curves towards larger particles. Nonetheless, qualitatively, the above conclusions are valid for the rough-rolled material as well.

Thus, with a view to the aim of the present study to speed up recrystallisation during self-annealing of the coiled hot strip, it appears that maximum recrystallisation rates require a two-stage homogenisation treatment as detailed above: (i) the material is annealed for a rather

short time of the order of 6 h at a high temperature, preferably above 560°C (yet still below the alloy's solidus temperature of ~580°C). This first anneal is intended to dissolve as many as possible of the fine intermetallic particles while avoiding deleterious grain boundary precipitation. (ii) Then, in preparation for hot rolling, the material is slowly cooled in the furnace to a temperature ranging from 400 to 500°C. During this second anneal, the matrix is depleted of solutes by growth of the remaining phases, resulting in the desired coarsened distribution of fairly large particles (Fig. 9b).

Interestingly, Zaidi and Sheppard, [3] describe the opposite behaviour, in that samples that were air cooled from soaking temperature recrystallised *faster* than furnace cooled ones. However, their samples were homogenised for 24 h at 600°C, i.e. above the alloy's solidus temperature, a practice which obviously results in a much more complete dissolution of second phases. Thus, it may be speculated that slow cooling of such a highly supersaturated structure may lead to a less suitable, much finer precipitation state than the two-stage homogenisation practice described in the present paper.

5. Conclusions

The factors affecting the microstructure development of the Al-Mg-Mn alloy AA5454 have been assessed with particular attention to the effects of homogenisation practice. Samples of both as cast and rough rolled transfer bar have been examined. The precipitation-dissolution behaviour of the alloy has been studied using DSC, DTA and electrical conductivity measurements. The effect of variations in the homogenisation practice have been observed by transmission electron microscopy and experimental rolling trials. A new, two-stage homogenisation practice is proposed which is designed to dissolve as much as possible of the fine second phase particles which retard recrystallisation by pinning grain boundaries.

Application of the two-stage homogenisation practice leads to enhanced recrystallisation behaviour following simulated tandem rolling. This process, now adopted industrially, leads to greater degrees of recrystallisation during self annealing, with associated benefits to the customer in terms of the ductility and formability of the alloy.

Table 1: Average composition of the present material and AA standard chemical composition of alloy AA 5454, in wt%.

Element		Mg	Mn	Fe	Si	Cr	Cu	Zn	Ti	Al
Average composition		2.90	0.83	0.37	0.15	0.07	0.04	0.01	0.01	Bal.
AA specification	min	2.4	0.5			0.05				
	Max	3.0	1.0	0.4	0.25	0.2	0.1	0.25	0.2	Bal.

Table 2: Extreme values (minimum and maximum, wt%) of alloy composition along the cross section of the rough-rolled plate, *cf.* Table 1.

element		Mg	Mn	Fe	Si	Cr
mean composition		2.9	0.83	0.37	0.15	0.07
measured	min	2.69	0.81	0.32	0.12	0.068
	max	3.25	0.87	0.44	0.16	0.077

Table 3: Test matrix of parameters varied in the hot rolling trials.

sample	ε	$\dot{\varepsilon}$ [s^{-1}]	T_{hom} [°C]	t_{hom} [h]	cooling rate*	T_{roll} [°C]	$\tau_{50\%}^{325°C}$ [min]	$\tau_{50\%}^{345°C}$ [min]
A1	0.8	2.5	585	24	w.q.	400	48	11
A2	0.8	2.5	585	6	f.c.	400	20	7
A3	0.8	2.5	540	6	f.c.	400	53	26
A4	0.8	2.5	560	6	f.c.	400	33	11
A5	0.8	2.5	570	6	f.c.	400	25	10
A6	0.8	2.5	540	18	f.c.	400	51	11
A7	0.8	2.5	560	18	f.c.	400	23	9
A8	0.8	2.5	570	18	f.c.	400	20	8
A9	0.52	2.5	560	6	f.c.	400		50
A10	0.52	6.8	560	6	f.c.	400		27
A11	0.8	6.8	560	6	f.c.	400		11
B1	1.36**	5.0	560	6	f.c.	400	11	
B2	1.36**	5.0	540	6	a.c.	486		22

*w.q.: water quenched, a.c.: air cooled, f.c.: furnace cooled
** three passes

References

1. F. Ostermann: ‘Anwendungstechnologie Aluminium‘, 1998, Berlin, Springer-Verlag.
2. D. Wieser and E. Brünger: in Proc. ‘10th Aachen Colloquium Automobile and Engine Technology’, (ed. S. Pischinger and H. Wallentowitz), Vol. 1, 495-507; 2001, Aachen, Germany, fka Forschungsgesellschaft.
3. M.A. Zaidi and T. Sheppard: *Metals Technol*., 1984, **11**, 313-319.
4. T. Sheppard and N. Raghunthan: *Mater. Sci. Technol.*, 1989, **5**, 268-280.
5. H.D. Merchant and J.G. Morris: *Metall. Trans. A*, 1990, **21A**, 2643-2654.
6. O. Engler, I. Heckelmann, T. Rickert, J. Hirsch and K. Lücke: *Mater. Sci. Technol.*, 1994, **10**, 771-781.
7. J.H. Beynon and C.M. Sellars: *ISIJ Int.*, 1992, **32**, 359-367.
8. I. Miki, H. Kosuge and K. Nagahama: *J. Jap. Inst. Light Met*., 1975, **25**, 1-9.
9. J.G. Barlock and L.F. Mondolfo: *Z. Metallkd.*, 1975, **66**, 605-611.
10. P. Skjerpe: *Metall. Trans. A*, 1987, **18A**, 189-200.
11. M. Osman: ‘Effect of Thermo-mechanical Treatments on the Recrystallisation Behaviour of the high Strength Al-Mg-Mn-Fe Alloy Type-5454’, PhD dissertation, 2002, Univ. of Strathclyde, Glasgow.
12. D. Altenpohl: ‘Aluminium und Aluminiumlegierungen’, 1965, Berlin, Springer-Verlag.
13. L. Kaufman and H. Bernstein: ‘Computer Calculation of Phase Diagrams with Special Reference to Refractory Materials‘, 1970, New York, Academic Press.
14. N. Saunders and A.P. Miodownik: ‘CALPHAD (Calculation of Phase Diagrams): A Comprehensive Guide’, 1998, Oxford, Pergamon.
15. C.W. Bale, P. Chartrand, S.A. Degterov, G. Eriksson, K. Hack, R. Ben Mahfoud, J. Melançon, A.D. Pelton and S. Petersen, *CALPHAD*, 2002, **26**, 189-228.
16. I. Ansara, A.T. Dinsdale and M.H. Rand: ‘Thermochemical Database for Light Metal Alloys’, 1998, European Commission, COST 507 V2 Final Report.
17. N. Saunders: *J. Jap. Inst. Light Met.*, 2001, **51**, 141-150.
18. F.J. Humphreys: *Acta metall*. 1977, **25**, 1323-1344.
19. C. Zener, quoted in C.S. Smith: *Trans. Met. Soc. AIME*, 1948, **175**, 15-51.
20. R.D. Doherty and J.W. Martin, *J. Inst. Metals*, 1962-63, **91**, 332-338.
21. H. Ahlborn, E. Hornbogen, and U. Köster: *J. Mater. Sci.,* 1969, **4**, 944-950.
22. H.E. Vatne, O. Engler and E. Nes: *Mater. Sci. Technol.*, 1997, **13**, 93-102.
23. K. Lücke and H.P. Stüwe: *Acta Metall*., 1971, **19**, 1087-1099.
24. F.J. Humphreys and M. Hatherly: ‘Recrystallisation and Related Phenomena’, 1995, Oxford, Pergamon.
25. H. Westengen: *Z. Metallkd*., 1982, **73**, 360-368.
26. A.L. Dons: *Z. Metallkd.*, 1985, **76**, 609-612.
27. E. Scheil: *Z. Metallkd.*, 1942, **34**, 70-72.
28. K. Sjølstad, O. Engler, S. Tangen, K. Marthinsen and E. Nes: *Mater. Sci. Forum*, 2002, **396-402**, 463-468.

Figure Captions

Fig. 1. Analysis of the distribution of the alloying elements along the cross section of the rough-rolled plate. (a) Schematic drawing for the plate cross section showing the area used in analysing the element distribution; (b) spatial distribution of Mg; (c) spatial distribution of Cr.

Fig. 2. Thermal analysis of the alloy AA 5454. (a) DSC analysis for the as-cast material (outer regions) and (b) DTA analysis of two positions of the rough-rolled slab representing maximum and minimum chemical heterogeneity.

Fig. 3: Impact of a homogenisation at a temperature of 600°C (i.e. above the solidus temperature), showing brittle phases on the grain boundaries with subsequent crack initiation (a) after homogenisation and (b) after hot rolling.

Fig. 4. Results of electrical conductivity measurements after heat treatment under various conditions. The solid line represents the equilibrium conductivity predicted by Eq. 2. The solid squares represent samples which underwent two-stage treatments consisting of a 6h homogenisation at 570°C, followed by furnace cooling to a temperature represented by their position on the x-axis and subsequent holding at that temperature for 3h before water quenching.

Fig. 5: TEM micrographs showing the evolution of secondary precipitates well away from the large constituents during homogenisation of the DC cast ingot. (a) as-cast slab, as received, (b) as cast slab after homogenisation at 540°C.

Fig. 6. Recrystallisation kinetics $X(t)$ of rough-rolled AA 5454 for two different cooling rates and annealing temperatures, T_{RX} (ε=0.8, $\dot{\varepsilon}$=2.5/s, T_{hom}=585°C, T_{roll}=400°C, see Table 3).

Fig. 7: Schematic temperature / time cycle of the various pre-heating practices, including furnace cooling (f.c.), air cooling (a.c.) and water quenching (w.q.) from homogenisation temperature, T_{hom}, to rolling temperature, T_{roll}.

Fig. 8: Time for 50% recrystallisation, $\tau_{50\%}$, plotted *vs*. the homogenisation temperature, T_{hom}, for two different homogenisation times, t_{hom}, and annealing temperatures, T_{RX}.

Fig. 9: Comparison between the precipitate states resulting from two different homogenisation treatments. (a) single stage homogenisation, (b) double stage homogenisation.

Fig. 10: Microstructure of a slabs of material, homogenised at 540°C for 6 hours (one-stage homogenisation), air cooled to 400°C, rolled for three passes with total strain of 1.36, and annealed for 60 minutes at 345°C. (a) As rough rolled material, (b) as cast material.

Fig. 11: TEM micrograph of an unrecrystallised region of the specimen shown in Fig. 10, showing interaction of second-phase particles with dislocations and subgrain boundaries.

Fig. 12: Microstructure of a slab of as-rough-rolled material, homogenised at 560°C for 6 hours, furnace cooled to 400°C (two-stage homogenisation), rolled for three passes with total strain of 1.36, and annealed for 60 minutes at 325°C.

Fig. 13: *FactSage* thermodynamic computations for alloy AA 5454 showing mass fraction x_i of the various phases as a function of temperature T. (a) equilibrium, (b) Scheil solidification simulation.

Fig. 14: Evolution of the particle size distribution during single and double-stage homogenisation. (a) as-cast, (b) rough-rolled.

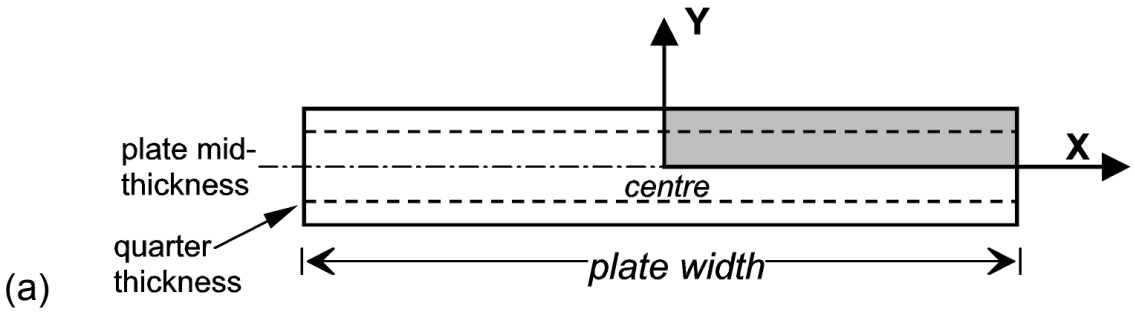

(a)

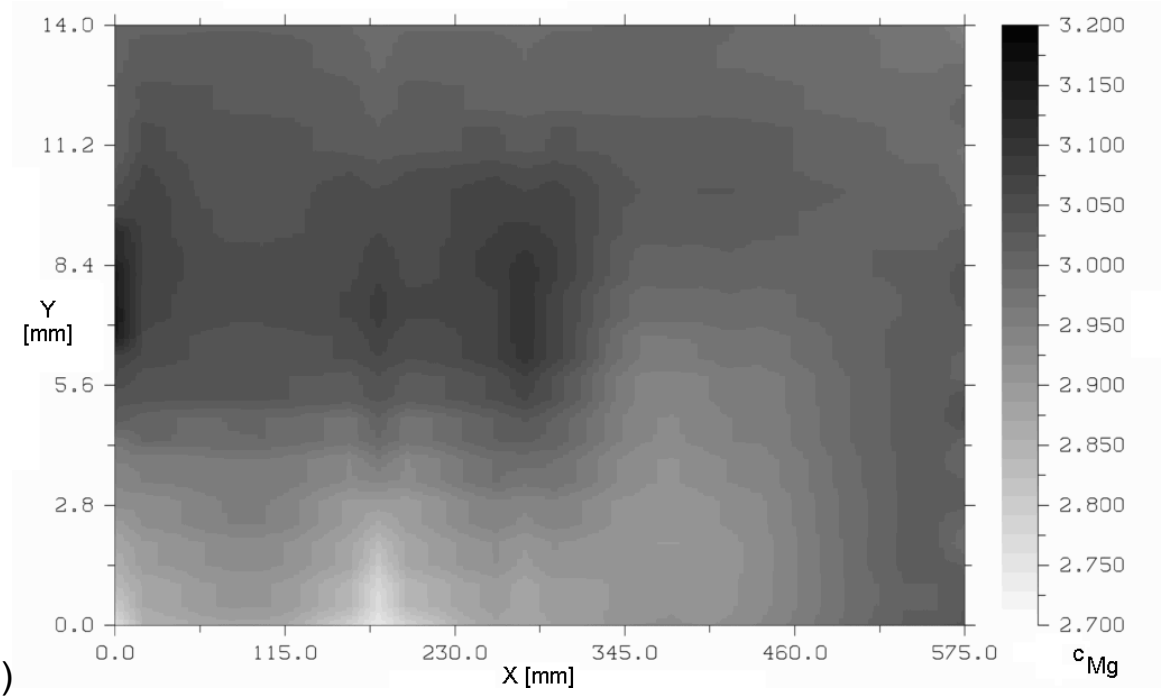

(b)

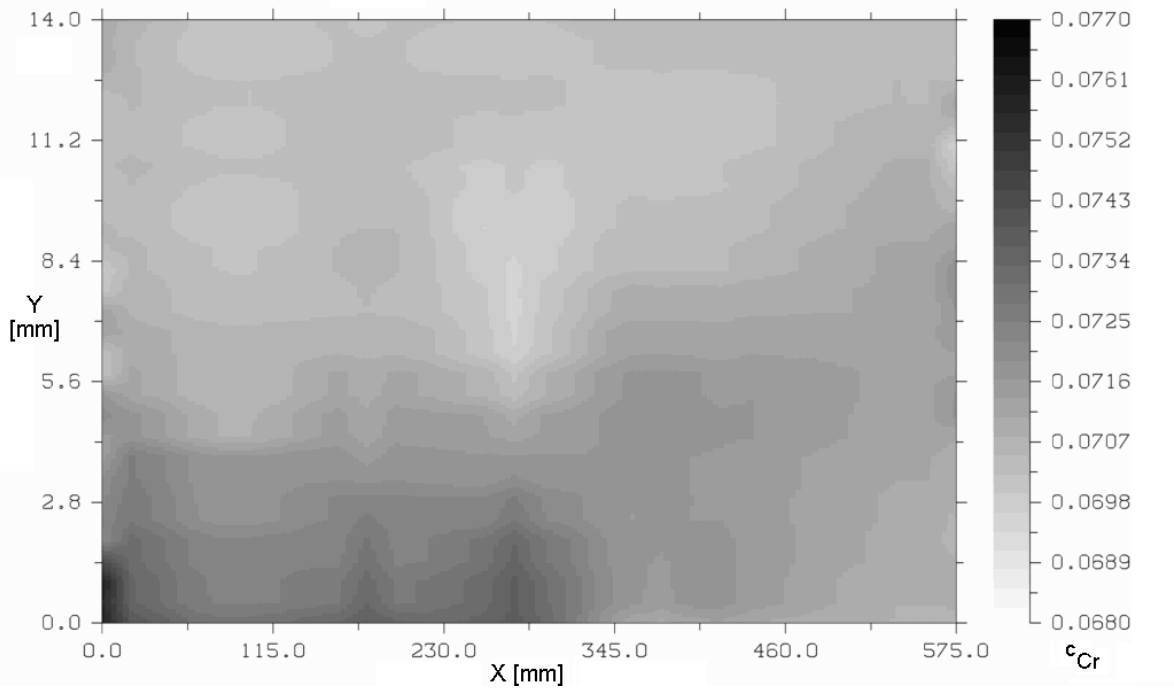

(c)

Osman et al., Fig. 1

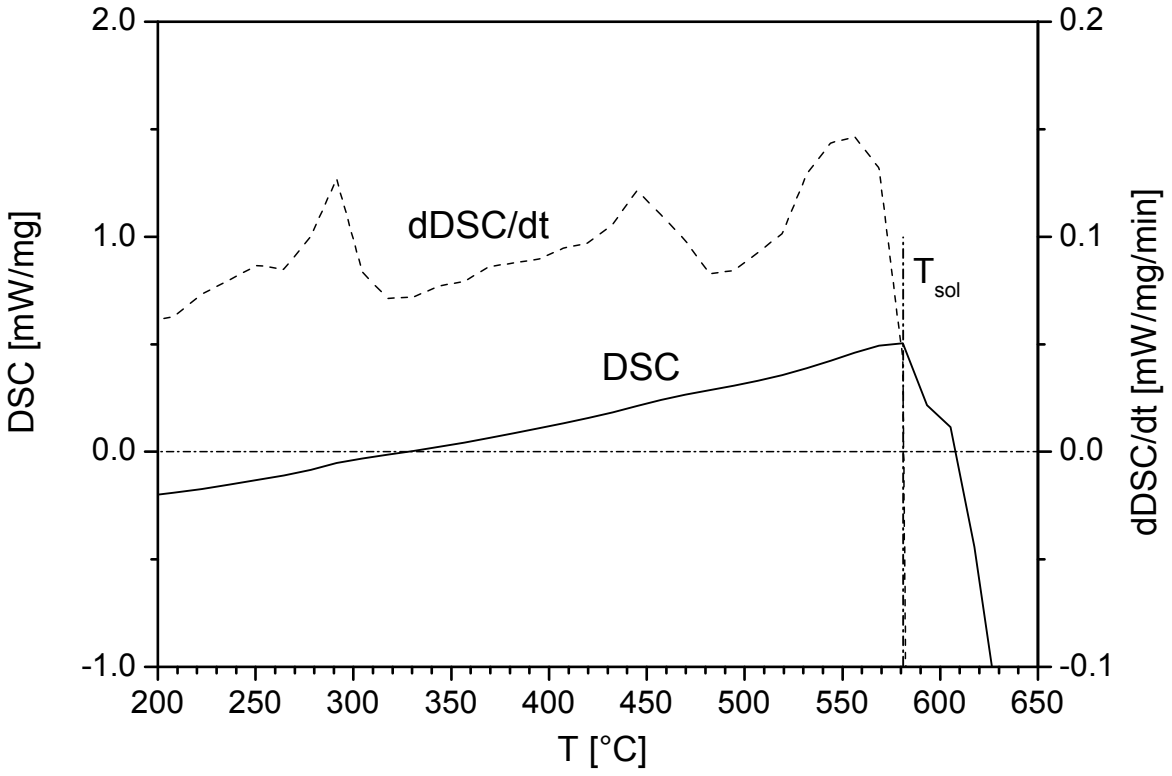

(a)

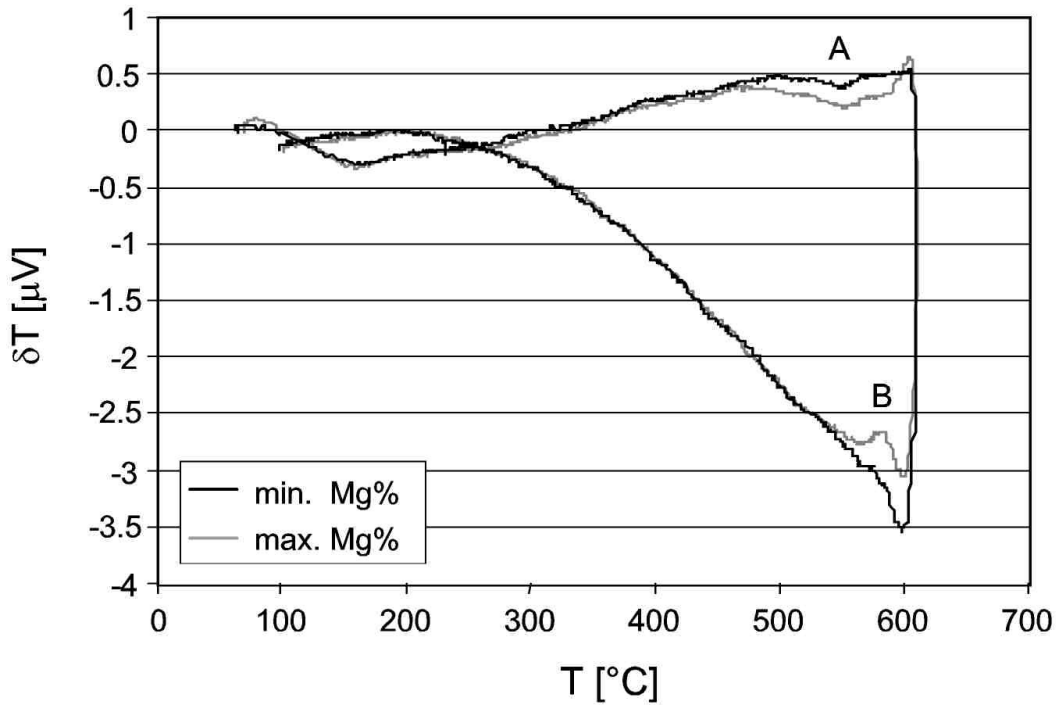

(b)

Osman et al., Fig. 2

(a)

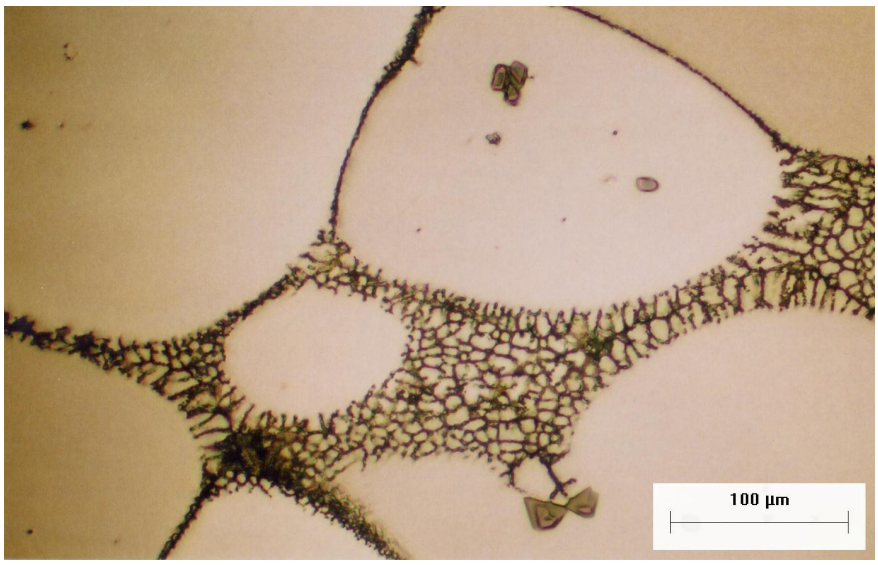

(b)

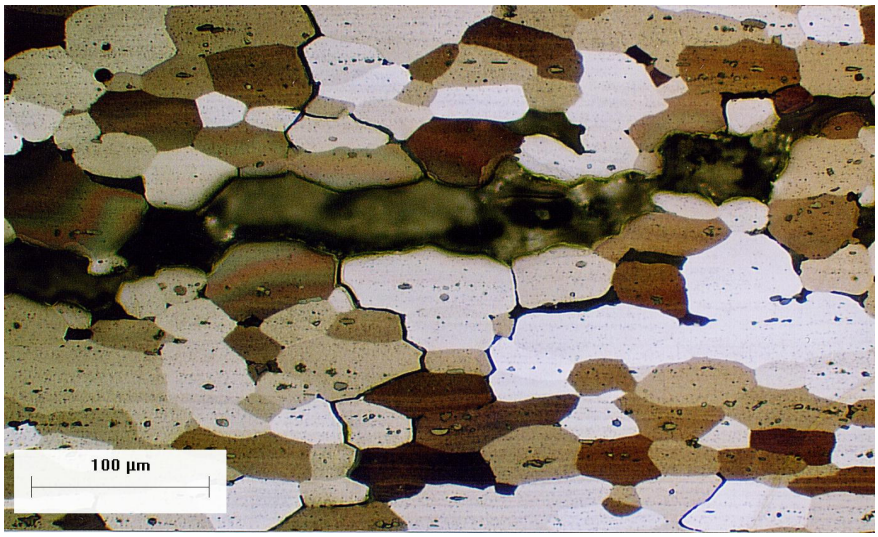

Osman et al., Fig. 3

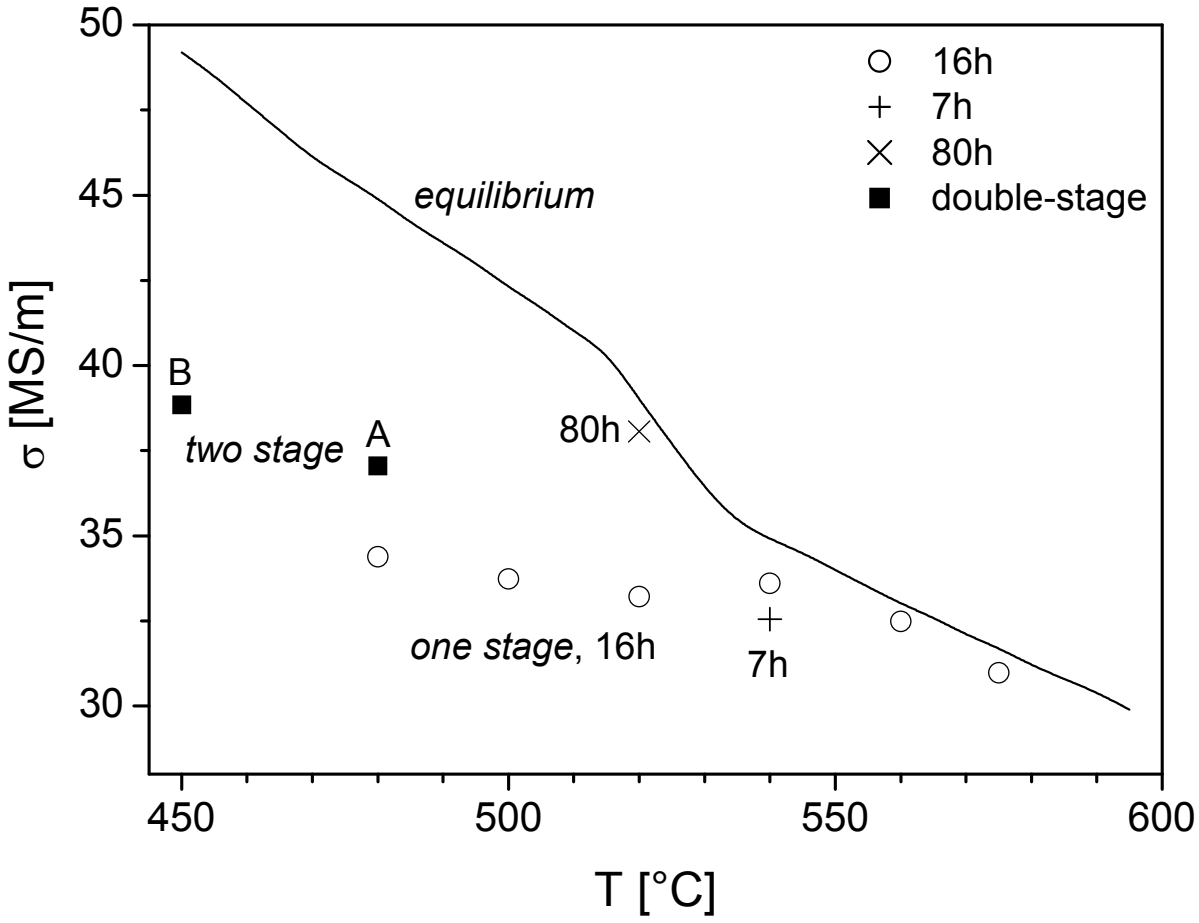

Osman et al., Fig. 4

(a)

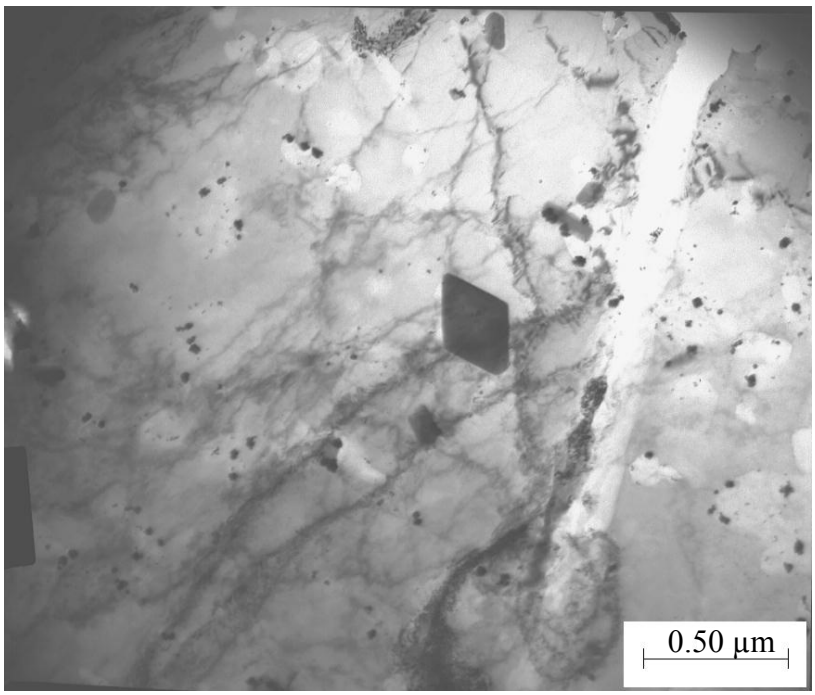

(b)

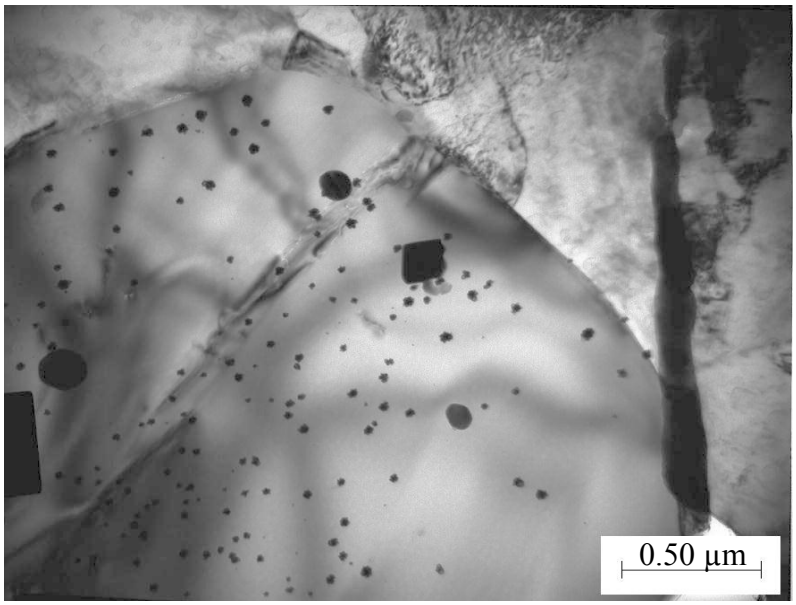

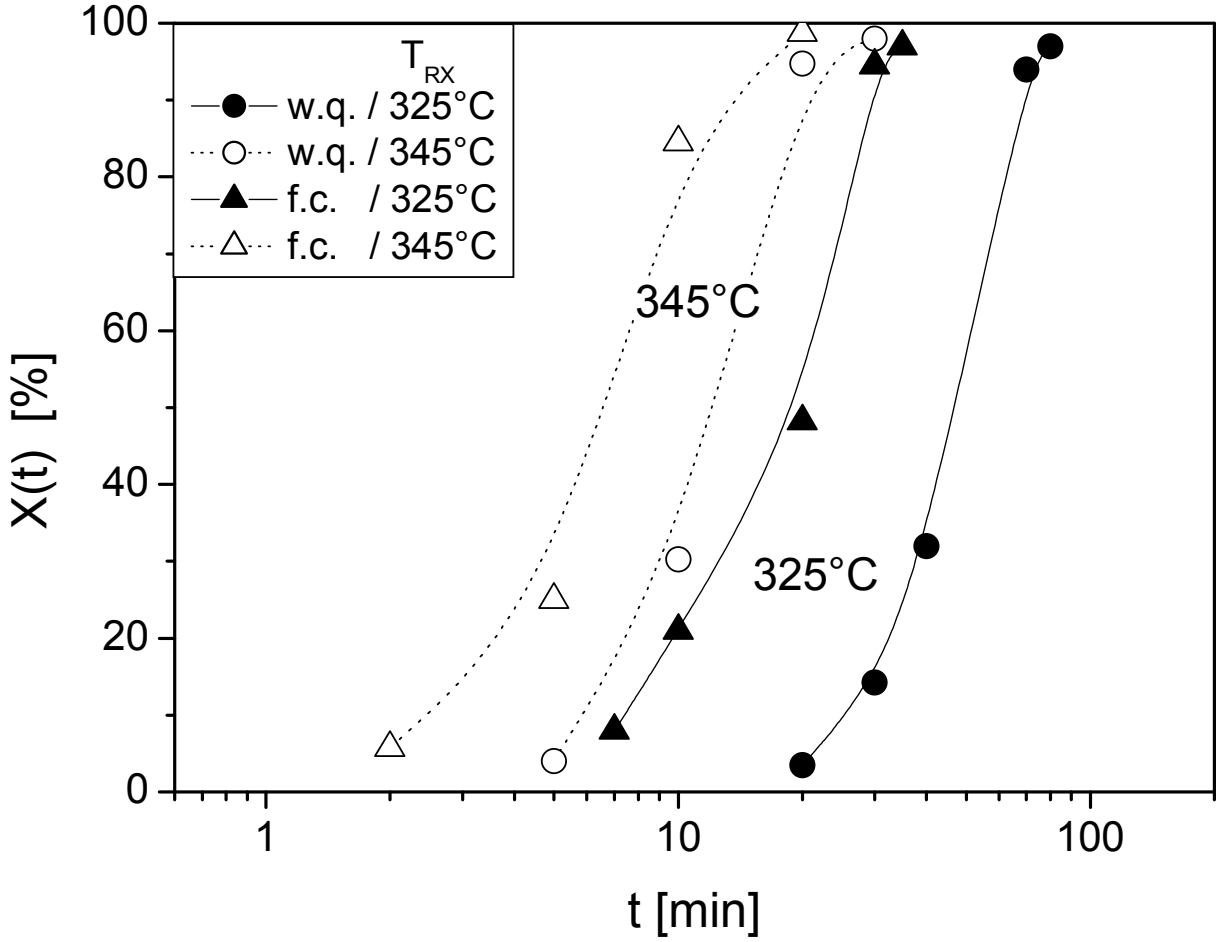

Osman et al., Fig. 6

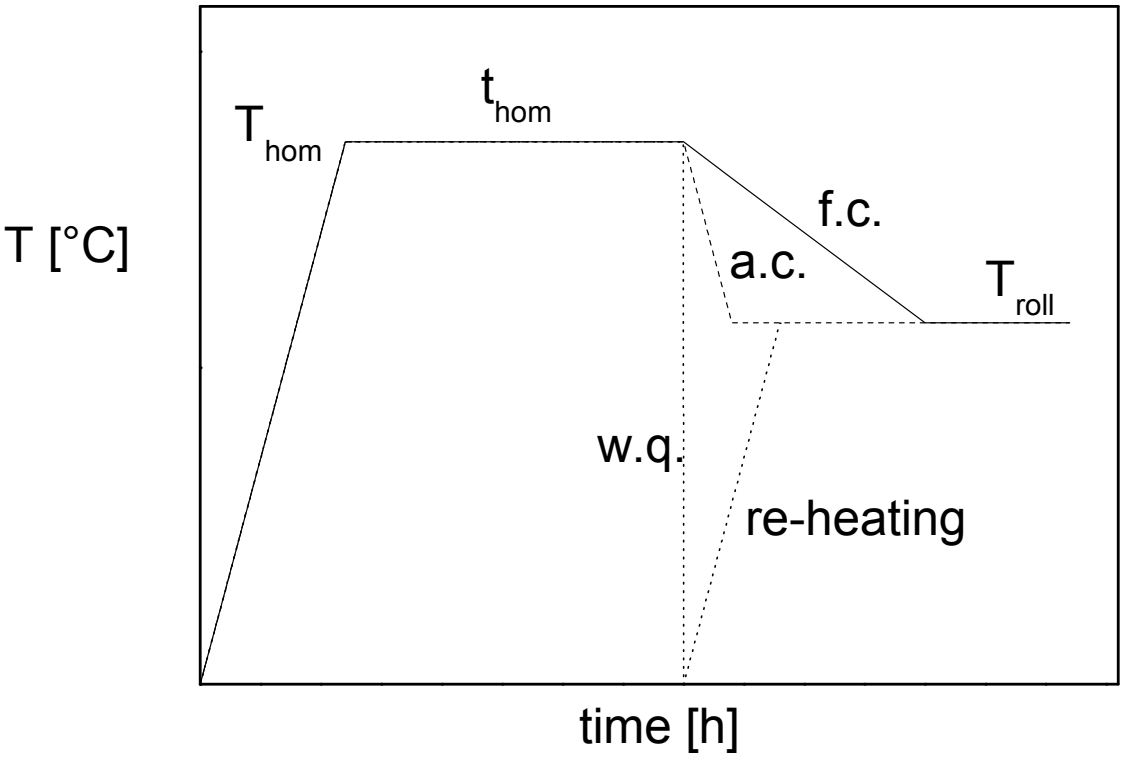

Osman et al., Fig. 7

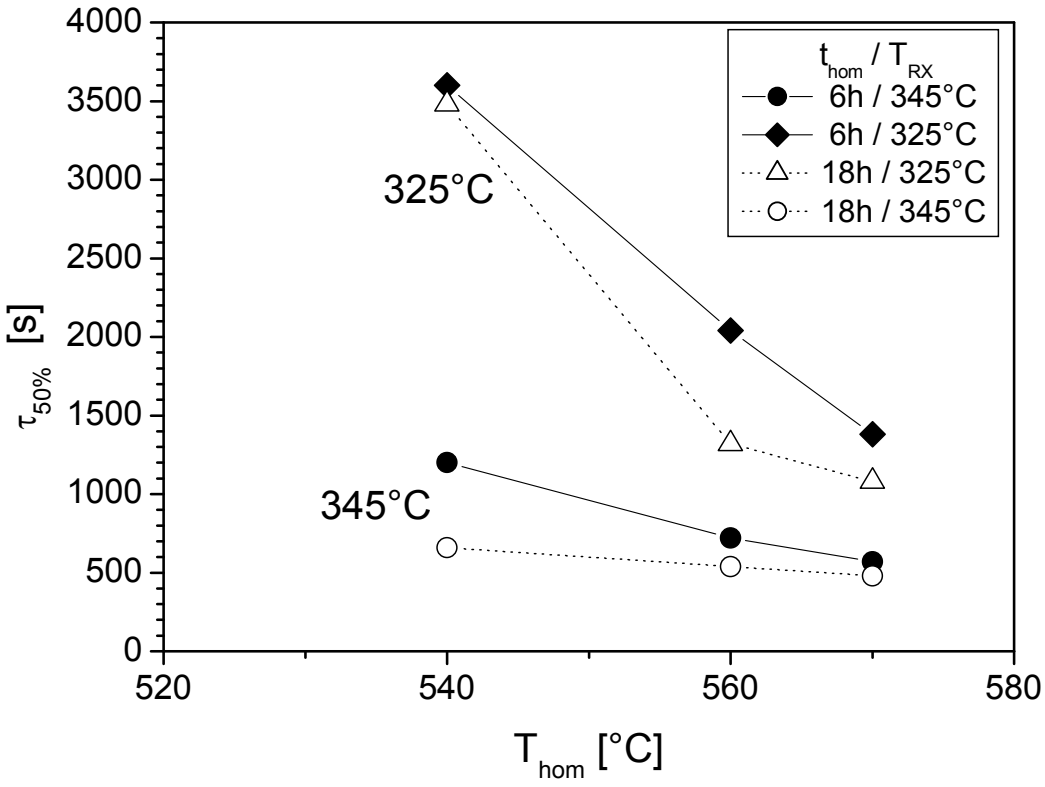

Osman et al., Fig. 8

(a)

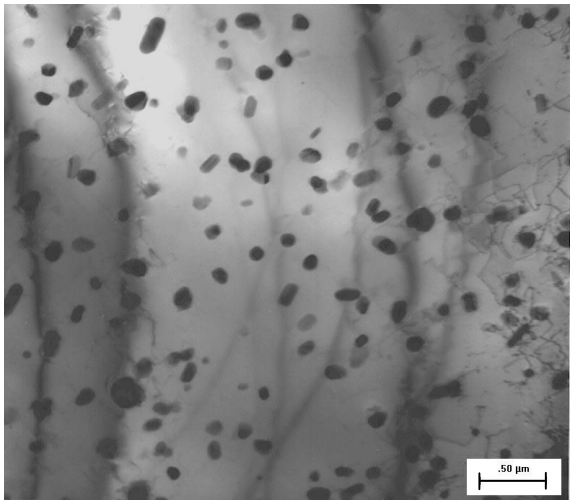

(b)

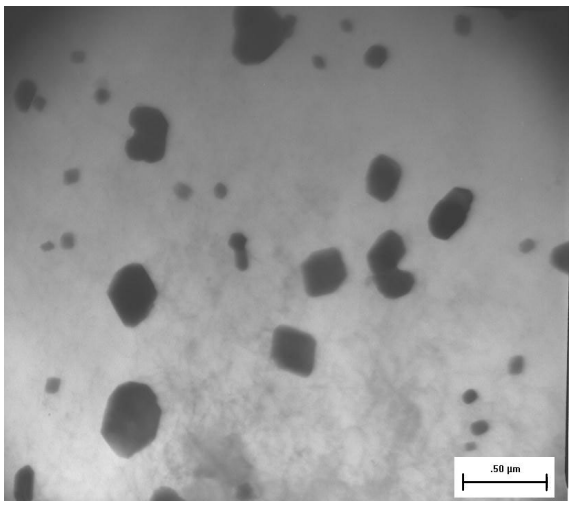

Osman et al., Fig. 9

(a)

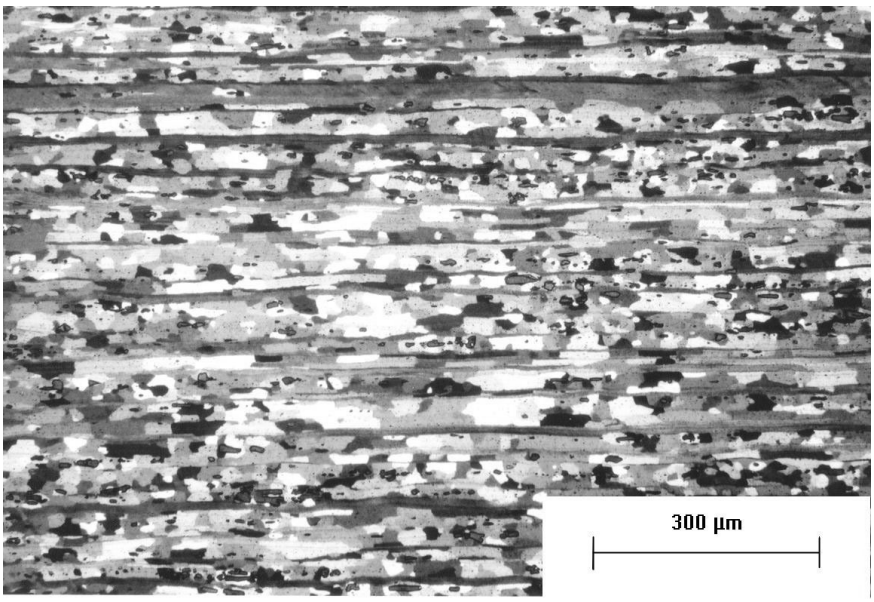

(b)

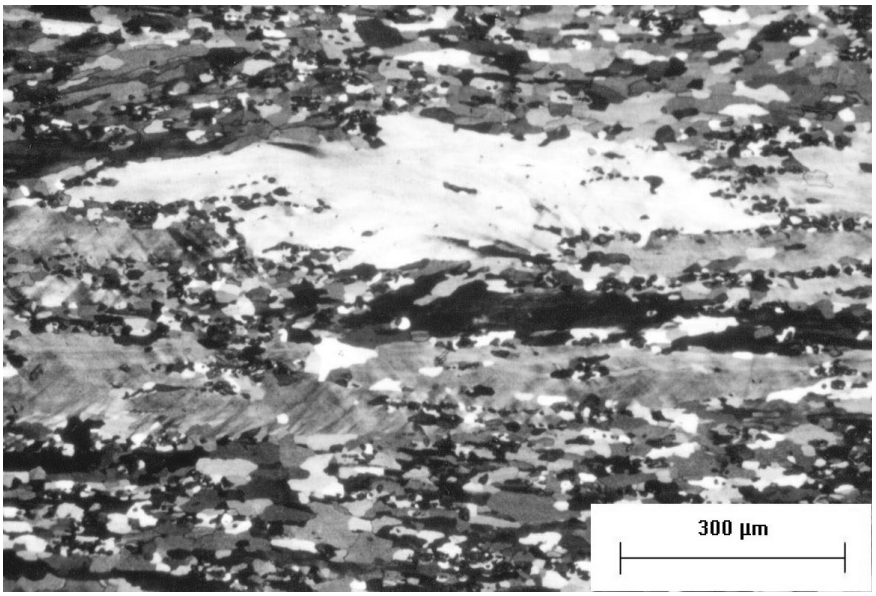

Osman et al., Fig. 10

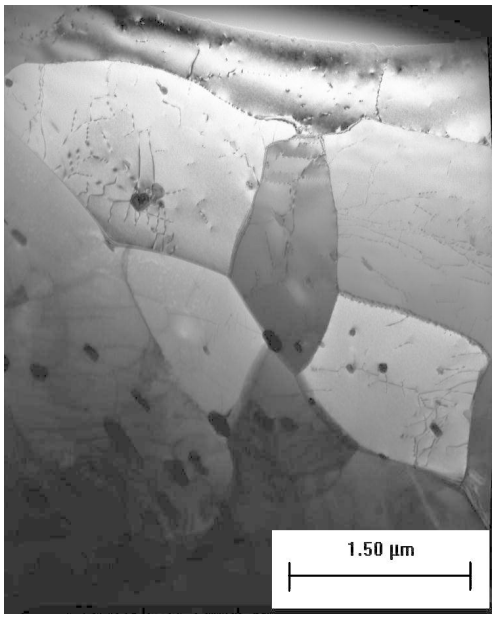

Osman et al., Fig. 11

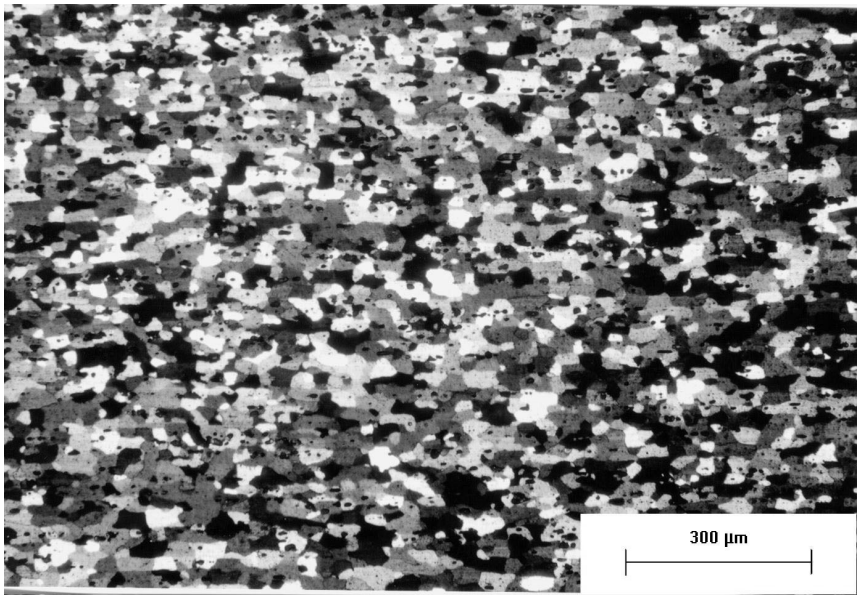

Osman et al., Fig. 12

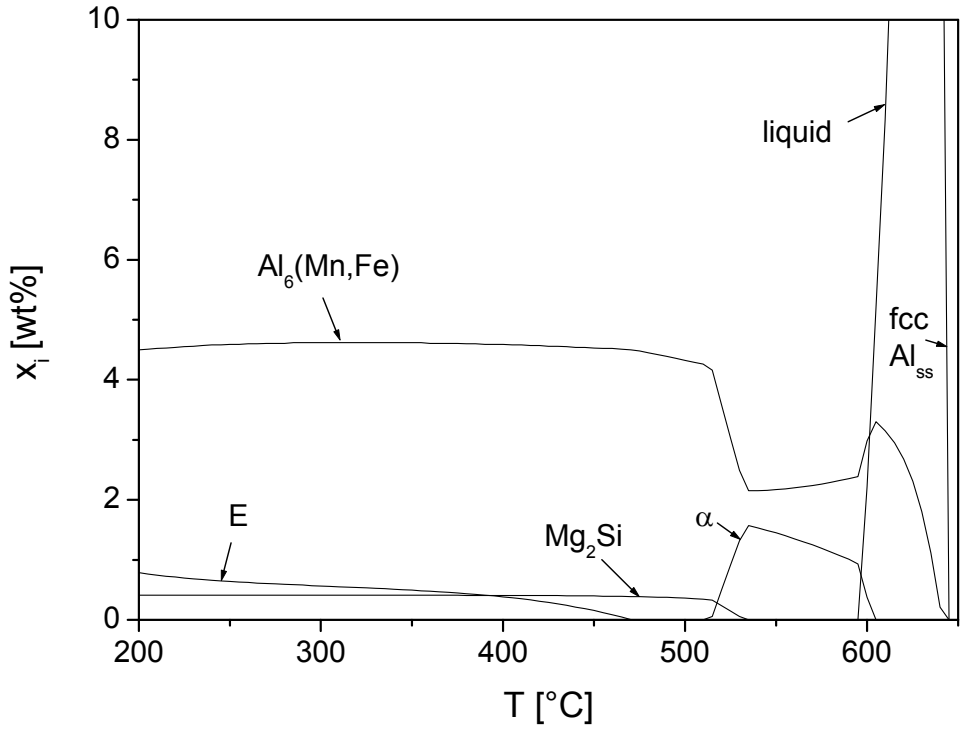

(a)

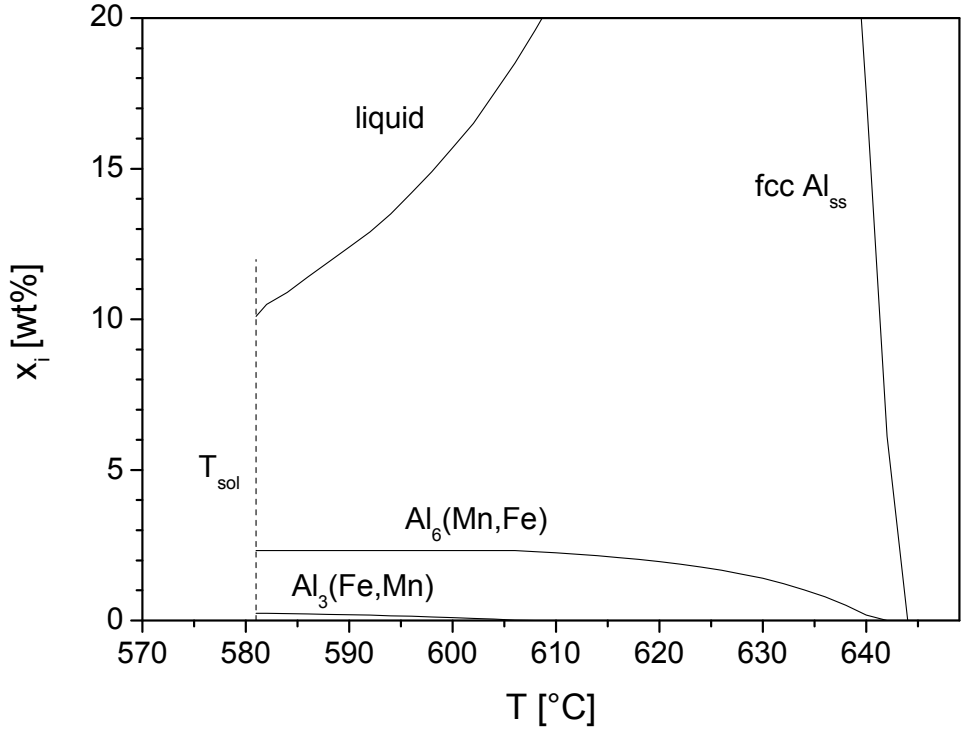

(b)

Osman et al., Fig. 13

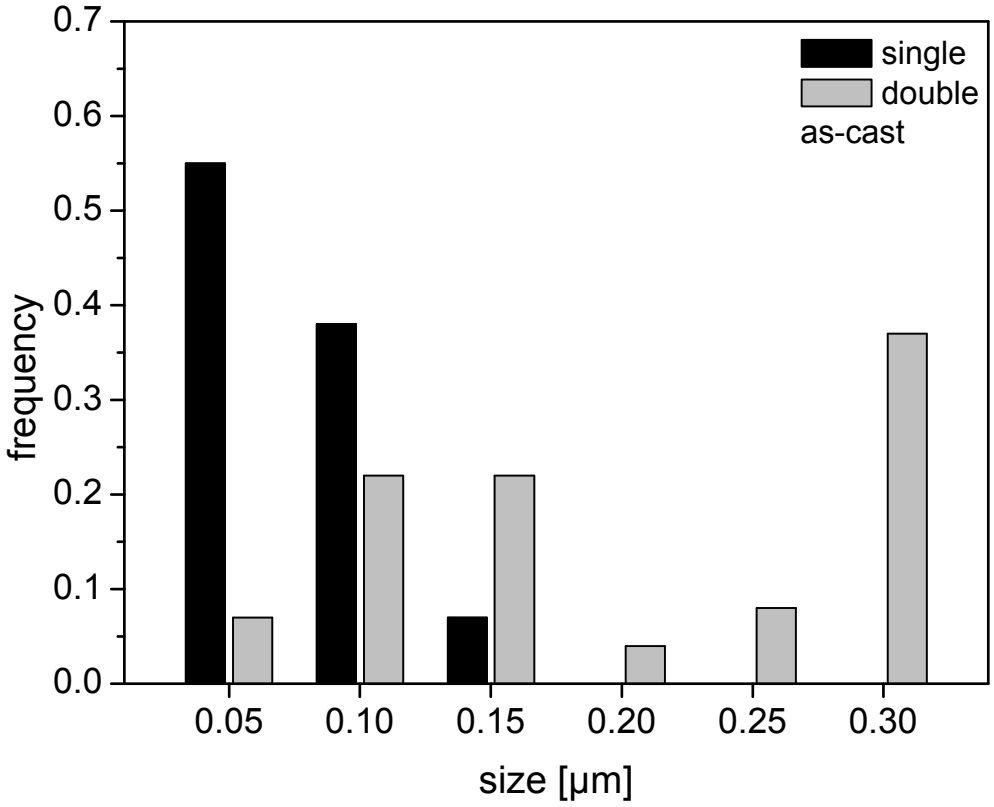
single
double
as-cast
frequency
0.0
0.1
0.2
0.3
0.4
0.5
0.6
0.7
0.05
0.10
0.15
0.20
0.25
0.30
size [μm]

(a)

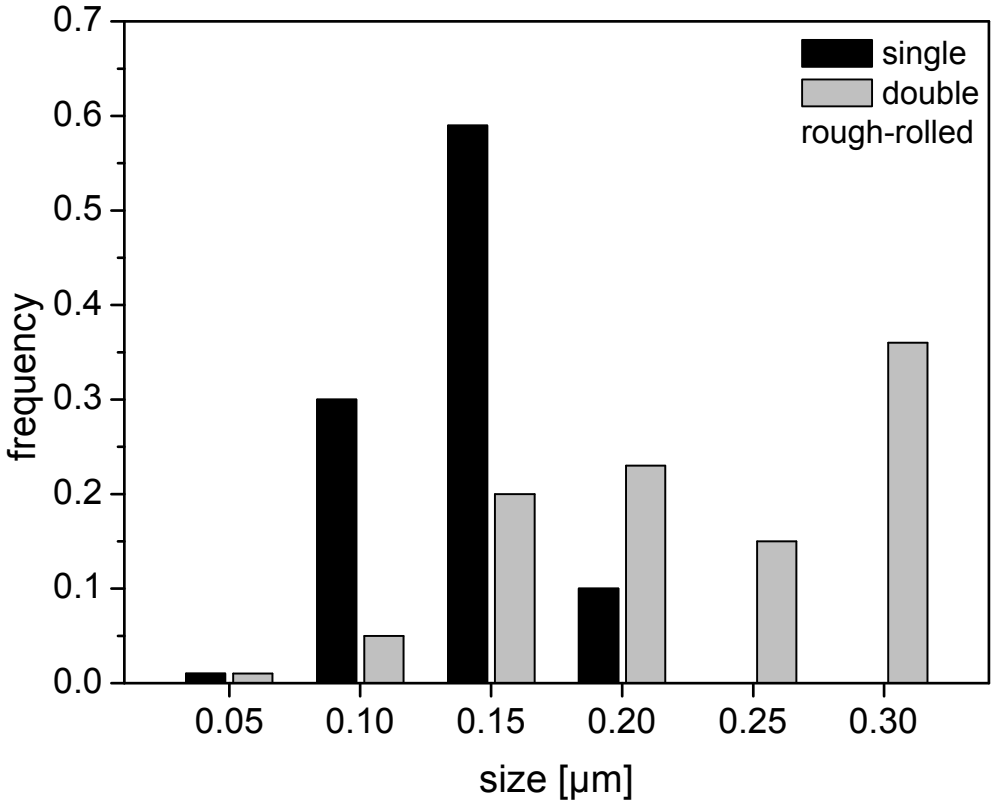
single
double
rough-rolled
frequency
0.0
0.1
0.2
0.3
0.4
0.5
0.6
0.7
0.05
0.10
0.15
0.20
0.25
0.30
size [μm]

(b)